Comparison of the Hinge Flow Fields of Two Bileaflet Mechanical Heart Valves under Aortic and Mitral Conditions

HÉLÈNE A. SIMON,[1] HWA-LIANG LEO,[2] JOSIE CARBERRY,[3] and AJIT P. YOGANATHAN[3]

[1]School of Chemical and Biomolecular Engineering, Georgia Institute of Technology, Atlanta, GA; [2]School of Mechanical Engineering, Georgia Institute of Technology, Atlanta, GA; and [3]Wallace H. Coulter Department of Biomedical Engineering, Georgia Institute of Technology, Atlanta, GA

Abstract—*Background:* Animal and clinical studies have shown that bileaflet mechanical heart valve designs are plagued by thromboembolic complications, with higher rates in the mitral than in the aortic position. This study evaluated the hinge flow dynamic of the 23 mm St. Jude Medical (SJM) Regent and the 23 mm CarboMedics (CM) valves under aortic conditions and compared these results with previous findings under mitral conditions. *Method:* Velocity and Reynolds shear stress fields were captured using two-component laser Doppler velocimetry. *Results:* Under aortic conditions, both the SJM and CM hinge flow fields exhibited a strong forward flow pattern during systole (maximum velocities of 2.31 and 1.75 m/s, respectively) and two main leakage jets during diastole (maximum velocities of 3.08 and 2.27 m/s, respectively). *Conclusions:* Aortic and mitral flow patterns within the two hinges were similar, but with a more dynamic flow during the forward flow phase under aortic conditions. Velocity magnitudes and shear stresses measured under mitral conditions were generally higher than those obtained in the aortic position, which may explain the higher rates of thromboembolism in the mitral implants when compared with the aortic implants.

INTRODUCTION

Bileaflet Mechanical Heart Valves

Since the first heart valve replacement in 1960, more than three million valves have been implanted worldwide. Mechanical heart valves have been used for more than two decades and remain the most widely implanted prosthetic heart valve design largely because of their unmatched durability. Although several mechanical and bioprosthetic heart valve designs are currently available, 75% of defective valves are replaced by bileaflet mechanical heart valves. When compared with other mechanical heart valves, bileaflet mechanical heart valves exhibit superior bulk flow hemodynamics, a larger orifice area, a lower transvalvular pressure drop, and fewer regions of flow stasis. Nevertheless, implantation of bileaflet mechanical heart valves may cause major complications including hemolysis, platelet activation, and thromboembolic events.

Hinge Importance

An inherent feature of bileaflet mechanical heart valves is the hinge recesses about which the leaflets pivot. Valve designs deliberately include a degree of leakage flow upon valve closure to wash out these recesses, prevent flow stasis and thus minimize blood element buildup. However, this flow which is driven through the narrow hinge regions by a large cross-valvular pressure gradient produces elevated flow velocities and high Reynolds shear stresses that may lead to hemolysis and initiation of the coagulation cascade. In-depth studies have shown that the flow fields within the constricted hinge region are critical to the proper function of the valves, since the hinge geometry directly influences the valve durability, functionality, fluid dynamics, and thrombus formation.[16]

Previous Hinge Studies

Medtronic Valve

The importance of the flow field through the hinge region to valve performance was emphasized by the unsuccessful clinical trials of the Medtronic Parallel (MP) bileaflet heart valve. This valve exhibited unacceptably high rates of thrombus formation upstream of and in the hinge region. Subsequent investigations have shown that the sudden expansion and contraction zones characteristic of the MP valve hinge recess give rise to unsteady flow, vortex, and stagnation regions, which could inhibit the washing of the pivot region and thus contribute to thrombus formation.[3,7] Additionally, these flow conditions were found to be associated with Reynolds shear stresses up to 8,000 dyn/cm^2,

Address correspondence to Ajit P. Yoganathan, Associate Chair, Wallace H. Coulter Department of Biomedical Engineering, Georgia Institute of Technology, 313 Ferst Drive, BME Building, Room 2119, Atlanta, GA 30332-0535. Electronic mail: ajit.yoganathan@bme.gatech.edu

which isgreater than the accepted threshold level of blood cell damage.[3,10,12,17]

In contrast to the MP valve, the St. Jude Medical (SJM) and the CarboMedics (CM) bileaflet mechanical heart valves have exhibited low thrombosis rates and good clinical performances and are currently the two most commonly implanted prosthetic heart valves.

St. Jude Medical Valve

The SJM valve has presented very low long-term rates of thrombosis and valve related complications, and hence remains today the most clinically successful bileaflet design. The SJM hinge geometry is characterized by a streamlined butterfly geometry with smooth contours, which minimize flow separation and stagnation, thus reducing levels of mechanically induced thromboembolic events. A previous investigation of the 25 mm SJM standard design under mitral conditions by Ellis showed that the highest peak leakage velocity and Reynolds shear stress reached 3.42 m/s and 7,400 dyn/cm[2,4] whereas the highest peak leakage velocity and Reynolds shear stress recorded within the hinge of the 23 mm SJM Regent design under mitral conditions were 1.52 m/s and 2,600 dyn/cm^2, respectively.[5] Additionally, the SJM valve design incorporates an expansion region downstream of the hinge mechanism called the thumbnail. Studies of the thumbnail region under mitral conditions have shown that this region is characterized by a skewed forward flow bounded by two recirculation zones. The inherently unsteady nature of the pulsatile flow and the complex flow field through the thumbnail region is believed to minimize blood element buildup.[5,6]

CarboMedics Valve

The second most widely used valve is the CM bileaflet mechanical heart valve. The CM valve has proved to be highly reliable as evidenced by no mechanical failure, valve dysfunction, or structural deterioration and a low incidence of valve related complications.[1] A study by Minakata[11] found that the CM valve demonstrates satisfactory clinical performance early on and acceptable mid-term performance. The CM hinge is characterized by an angulated recess and a butterfly geometry design with sharper corners and less streamlined edges than the SJM hinge design. Consequently, the projections of the leaflets within the recess cannot sweep the entire hinge area. A previous investigation by Leo[9] of the 23 mm CM under mitral conditions found that the highest peak leakage velocity and Reynolds shear stress were 3.17 m/s and 5,640 dyn/cm^2, respectively. The hinge hemodynamic performance of the 23 mm CarboMedics was demonstrated to be between those of a 27 mm MP and a 23 mm SJM Regent valves.
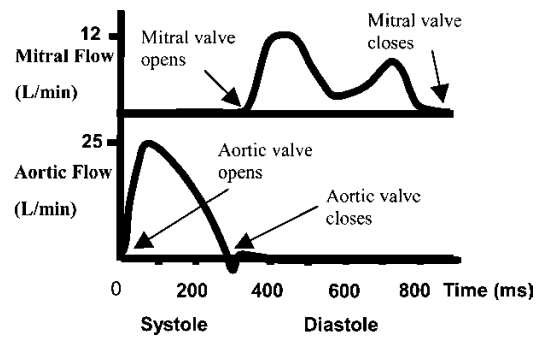

FIGURE 1. Schematic of the flow conditions in the aortic and mitral positions.

Dependence on Implant Location

The transvalvular flow conditions directly affect the hinge flow field and the thromboembolic potential of a valve as the leakage flow is driven by the cross-valvular pressure gradient. These flow conditions vary with the implant location. As shown in Fig. 1, valves implanted in the mitral position are not subjected to the same flow conditions as those in the aortic position, hence their clinical performances vary. Previous animal and clinical studies have revealed that thromboembolic complication rates are higher for valves implanted in the mitral position.[2,8,11,14] Therefore, clinical reports indicate that mechanical valves implanted in the aortic position have better performances than those implanted in the mitral position.

Aim of This Study

The present study investigates the hinge and near-hinge flow fields of the 23 mm SJM Regent and the 23 mm CM valves in the aortic position. The flow characteristics are then compared with previous findings in the mitral position in order to provide a better understanding of the dependence of the clinical performance upon implant location.

METHOD

Pulsatile Flow Loop

The valves were mounted in the aortic position of the Georgia Tech left heart simulator. The flow loop consisted of a pneumatic pulsatile system, a reservoir, an aortic valve-mounting chamber, a mitral valve-mounting chamber, resistance and compliance sections, a flow transducer, as well as ventricular and aortic pressure transducers. The compliance and resistance sections of the loop were adjusted to maintain the following conditions: heart rate of 70 beats/min, systolic duration of 300 ms, peak systolic flow rate of 25 L/min, cardiac output of 5 L/min, and aortic pressure of 80–140 mmHg. The resulting flow and pressure waveforms are shown in Fig. 2.

The flow rate was measured with a 24 mm in-line ultrasonic flow probe (model T108, Transonic Inc, Ithaca, NY)
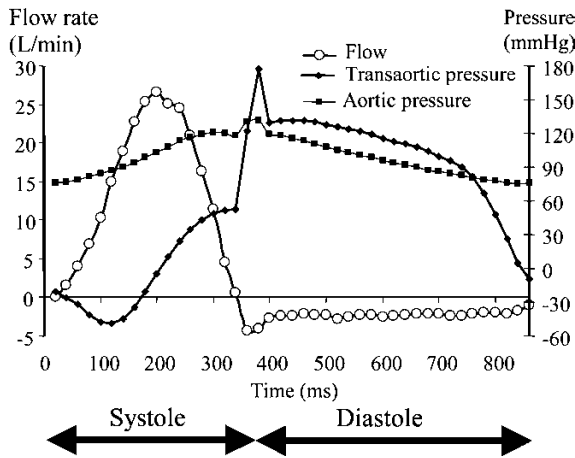
FIGURE 2. Aortic flow and pressure waveforms.

interfaced with a medical volume flow meter (CardioMed CM-4008, Medi-Stim AS, Norway). Aortic and ventricular pressures were measured with two pressure transducers (Model 43–272, Baxter Healthcare Corporation, Irvine, CA) interfaced with a Physiological Trace System (CardioMed CM-4008, Medi-Stim AS, Norway).

The working fluid was a solution of 79% saturated aqueous sodium iodide solution, 20% glycerin, and 1% water by volume. This blood analog fluid had a kinematic viscosity of 3.5 cSt to match that of blood at high-shear rates and its refractive index was matched to that of the valve-mounting chamber (1.49) to minimize optical distortion. The flow was seeded with neutrally buoyant silicon carbide particles (Model 10081, TSI Inc, St Paul, MN) with a nominal diameter of 1.5 μm.

Laser Doppler Velocimetry

Two-component velocity measurements were obtained with a three-component fiber-optic Laser-Doppler Velocimetry (LDV) system (Aerometrics Inc, Sunnyvale, CA) used in coincident backscattering mode. A 5 W multi-line argon-ion laser (Innova 70, Coherent, Santa Clara, CA) was coupled to a fiber drive unit to allow color separation of the incoming primary beam. The resulting green (514.5 nm wavelength) and blue (488 nm wavelength) beams were used for the two-component measurements. A Bragg cell was used to add a 40 MHz frequency shift to one beam of each color pair. A two-component transceiver (Model XRV 1204, TSI Inc, Shoreview, MN) with a 100 mm focal length lens was coupled to the fiber-optic couplers to produce an ellipsoidal measurement volume with minor and major axes of approximately 21 and 140 μm, respectively.

Clear Housing Valves

In order to gain optical access to the hinge regions, St. Jude Medical, Inc. provided a 23 mm SJM Regent clear housing valve, as well as a reverse-engineered clear housing cast of a clinical 23 mm CM bileaflet valve. The clear housing valves were high quality reproductions of the clinical valves. The tolerances were identical to those of clinical valves and the leaflets of both valves were manufactured from pyrolytic carbon.

Data Acquisition and Processing

The Doppler signals were processed with fast Fourier transform based real-time signal analyzers (Aerometrics, Model RSA1000 L, TSI Inc, Shoreview, MN) and a commercial software package (Aerometrics System Software, Particle Acquisition and Analysis, Version 0.80) was used to acquire data and control both the signal analyzers and the photomultiplier hardware. A resettable clock and a three-channel analog-to-digital converter were interfaced with the pulse duplicator to synchronize data acquisition with aortic flow and pressure waveforms. A total of approximately 21,500 measurements were taken at each location.

Data Reduction

Velocities and Reynolds shear stresses were obtained from the LDV data using the method outlined below. A more detailed description of data reduction can be found in the literature.[4,6,9,15] The velocities were phase-averaged within 20 ms time windows, each of which contained an average of 500 data points. Velocities were computed using a gate-time weighted averaging method to eliminate velocity bias. Statistical filtering was then applied and values more than five standard deviations away from the mean were discarded. The stress tensor and the principal Reynolds shear stress were calculated directly from the fluctuating velocity components at each measurement location and within every time bin. The principal time-averaged Reynolds shear stress provides an indication of the magnitude of the stress experienced by the blood cells traveling through the hinge regions and is referred as RSS in the remainder of this article.

Measurement Sites

In order to get a detailed representation of the flow within the hinge recess of the SJM Regent and CM clear housing valve models, measurements were performed at selected locations, which for purpose of comparison were similar to those chosen in previous hinge studies.[5,9] For the SJM hinge, the LDV measurement planes were located at the flat level and at 500, 1,000, and 3,000 μm below the flat level, as well as at 195, 390, and 585 μm above the flat level. A reduced number of measurement planes were considered for the CM valve, because its geometry does not include a thumbnail region: the flat level, 195 and 390 μm above the flat as well as 1,000 μm below the flat. Figure 3 shows top and elevated views of the measurement sites.

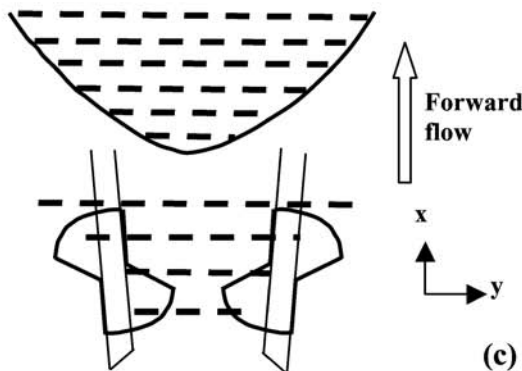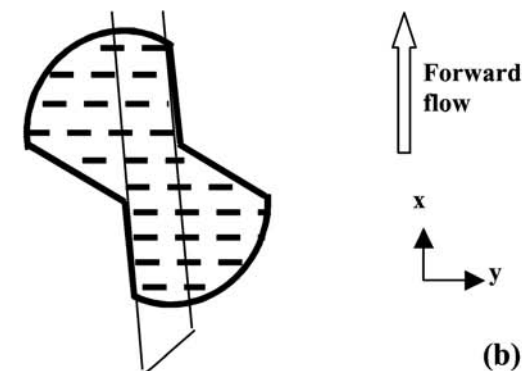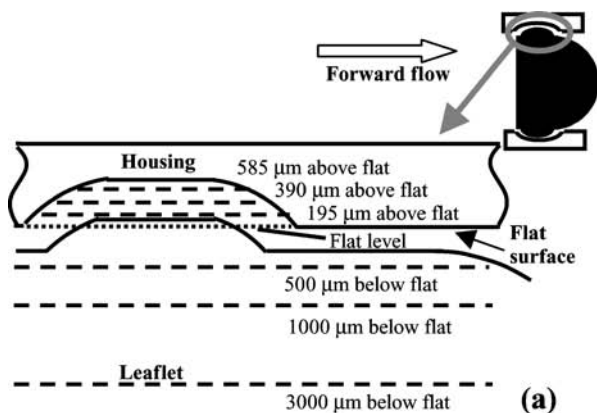At each measurement plane, the probe volume was manually positioned in a simple x–y grid pattern using a

FIGURE 3. Elevation view (a) and top views (b, c) of the LDV measurement sites within and in the vicinity of the hinge region. (a)The investigation of the CM valve design was limited to five planes, whereas seven elevations were investigated in the SJM Regent design due to the presence of a thumbnail region. (b) Measurements at the flat level and above were taken within the hinge recess of both mechanical valves. (c) Measurements below the flat level of the CM valve were taken over the two hinges, whereas measurements below the flat level of the SJM Regent valve were taken in the hinge region as well as in the thumbnail region.

traversing stage with an accuracy of 25.4 μm. The grid resolution for both hinge studies at and above flat level was 0.203 mm in the x and the y directions. Below the flat level, the grid spacing was 0.64 mm in both the x and y directions for the SJM Regent valve and was 1.06 and 0.41 mm in the x and y directions, respectively, for the CM valve.

RESULTS

The results are presented in the form of figures that illustrate the flow fields at specific instances of the cardiac cycle. In Figs. 5–9, the direction of the forward flow, from the left ventricle to the aorta, is oriented upwards. For clarity, the leaflets are not superimposed on the velocity flow fields. The arrows point in the direction of the mean velocity vectors and are color-coded by the velocity magnitude given in the figure legends. The arrow lengths are proportional to the velocity magnitude. Velocity scales vary from figures to figures. Terminology used to describe the geometry of the hinge is shown in Fig. 4.

Flat Level

Figure 5 shows the velocity fields at the flat level inside the CM and SJM hinges during mid-acceleration. In both hinge designs, a forward flow jet developed in the lateral corner traveling nearly parallel to the forward flow direction. The peak velocity magnitude in this region reached 1.75 and 2.31 m/s in the SJM and CM hinges, respectively. A peak RSS level of 1,113 dyn/cm^2 was found along the outflow wall of the SJM hinge, whereas in the CM hinge design, the RSS levels reached 5,690 dyn/cm^2 where the jet impinged upon the outflow wall.

In the SJM hinge, a slow counterclockwise rotating structure developed within the adjacent corner. Velocities up to 1.45 m/s and RSS levels up to 675 dyn/cm^2 were seen along the inflow wall. In the CM hinge, an S-shaped flow was observed in the adjacent corner with velocity magnitudes up to 2.24 m/s and near the inflow wall, the RSS levels reached 6,902 dyn/cm^2.

At peak systole, not shown, the velocity fields at the flat level were qualitatively similar to those observed during
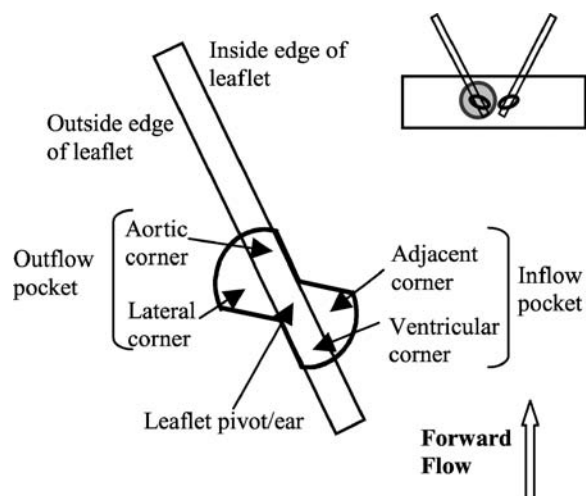

FIGURE 4. Pertinent terminology used to describe the SJM hinge flow field. Similar terminology was used for the description of the CM hinge flow field.
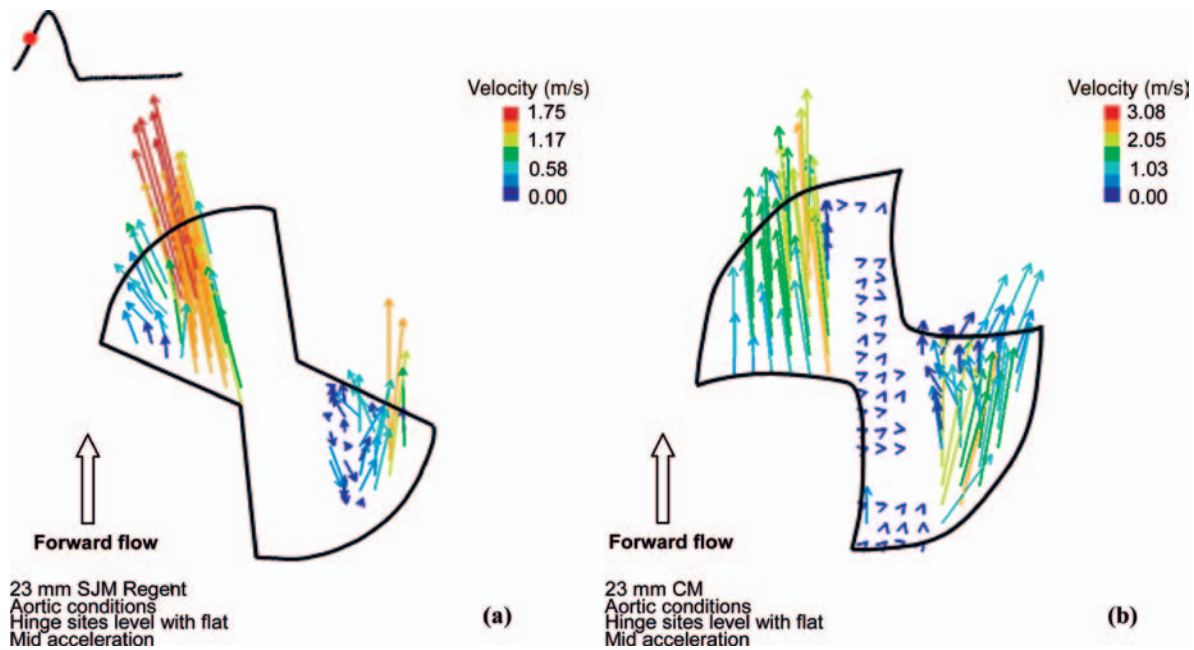
FIGURE 5. Hinge flow fields of the 23 mm SJM Regent valve (a) and of the 23 mm CM valve (b) placed in the aortic position at mid-systolic acceleration, at the flat level.

mid-acceleration, but the velocity magnitudes were lower. The peak velocities in the forward flow jet in the lateral corner were 1.27 and 1.39 m/s in the SJM and CM hinges, respectively. In the inflow pocket, the maximum velocities were 0.94 m/s in the SJM valve and 1.45 m/s in the CM valve. The peak RSS level was higher in the CM valve with a peak RSS of 2,880 and 478 dyn/cm^2 in the CM and SJM hinges, respectively.

As shown in Fig. 6, the rotating structure and the forward flow jet which characterized the flat level flow fields at mid-acceleration and peak systole were not observed at mid-diastole. At this instance of the cycle, a localized leakage jet with velocities up to 1.64 m/s was observed in the adjacent corner of the SJM valve. In the CM hinge design, the leakage flow reached velocities up to 3.08 m/s and expanded throughout the tip of the ventricular corner. High velocities were also recorded in the narrow region of the lateral corner between the hinge wall and the leaflet ear surface. In this corner, the velocities reached 0.9 and 1.42 m/s in the SJM and CM hinges, respectively. In both hinges, the highest RSS levels were recorded in the inflow pocket with a peak value of 5,440 dyn/cm^2 in the CM hinge and 2,657 dyn/cm^2 in the SJM hinge.

195 μm above the Flat Level

The forward flow velocity field at the 195 μm level, shown in Fig. 7, was significantly different from the corresponding flow field at the flat level, shown in Fig. 5. At the 195 μm level during mid-acceleration, there was no forward flow jet in the lateral corner, but a slow reverse flow was present with velocities up to 0.25 m/s in the SJM valve

and 0.47 m/s in the CM valve. A disturbed rotating structure with velocities up to 0.86 m/s was present in the adjacent corner of the SJM valve. In the CM valve design, the flow structure in the adjacent corner was similar to that seen at the flat level, and at early systole the velocities reached 1.55 m/s near the surface of the leaflet ear.

At peak systole, not shown, the general form of the flow field was similar to that seen during mid-acceleration, but the velocity magnitudes in the adjacent corner were slightly lower with peak velocities of 0.75 and 0.4 m/s in the CM and the SJM hinges, respectively. However, a peak velocity of 1.04 m/s was recorded in the disturbed inflow region of the SJM hinge.

At mid-diastole, not shown, the flow field was characterized by the presence of two main leakage jets and the velocity vectors throughout the hinge pointed nearly in the same directions as those seen at the flat level. In both designs, the maximum leakage flow velocities and RSS levels were recorded in the inflow pocket. The peak velocities reached 1.96 m/s in the SJM hinge and 2.57 m/s in the CM hinge, whereas the peak RSS levels were 5,460 dyn/cm^2 in the SJM valve and 6,192 dyn/m^2 in the CM hinge. The leakage flow observed in the lateral corner of the CM hinge was less localized at the 195 μm level than at the flat level. The reverse flow velocities in the outflow pocket reached 0.25 and 2.07 m/s in the SJM and CM hinges, respectively.

390 μm above the Flat Level

At mid-acceleration, not shown, a rotating structure was observed in the adjacent SJM corner, whereas in the CM hinge the flow field was more disturbed. In the adjacent
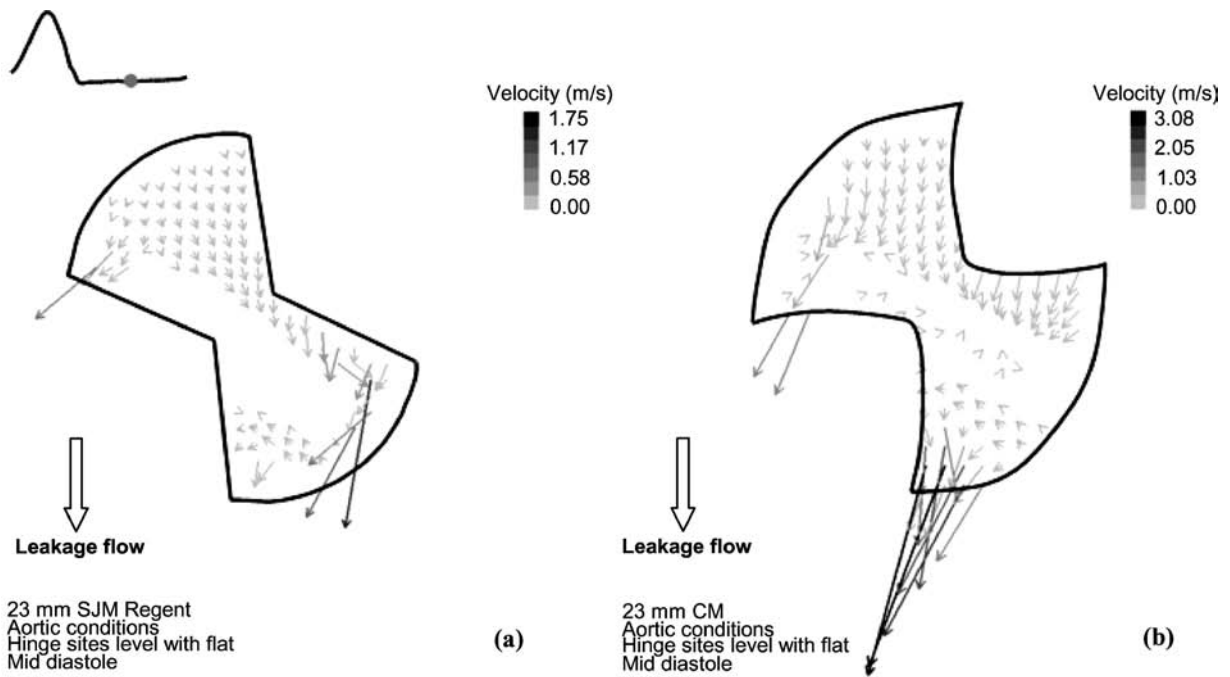
FIGURE 6. Hinge flow fields of the 23 mm SJM Regent valve (a) and of the 23 mm CM valve (b) placed in the aortic position at mid-diastole, at the flat level.

corner, the peak forward flow velocity was 1.07 m/s in the SJM hinge, whereas in the CM hinge, the velocities reached 0.73 m/s at early systole, and decreased to 0.39 m/s at mid-acceleration. The outflow pocket was characterized by low velocity flow with velocity magnitudes up to 0.40 m/s in

the SJM valve design and up to 0.21 m/s in the CM valve design.

At peak systole, not shown, the flow pattern within both hinges remained similar to those seen at mid-acceleration, but the velocity magnitudes were lower with peak velocities
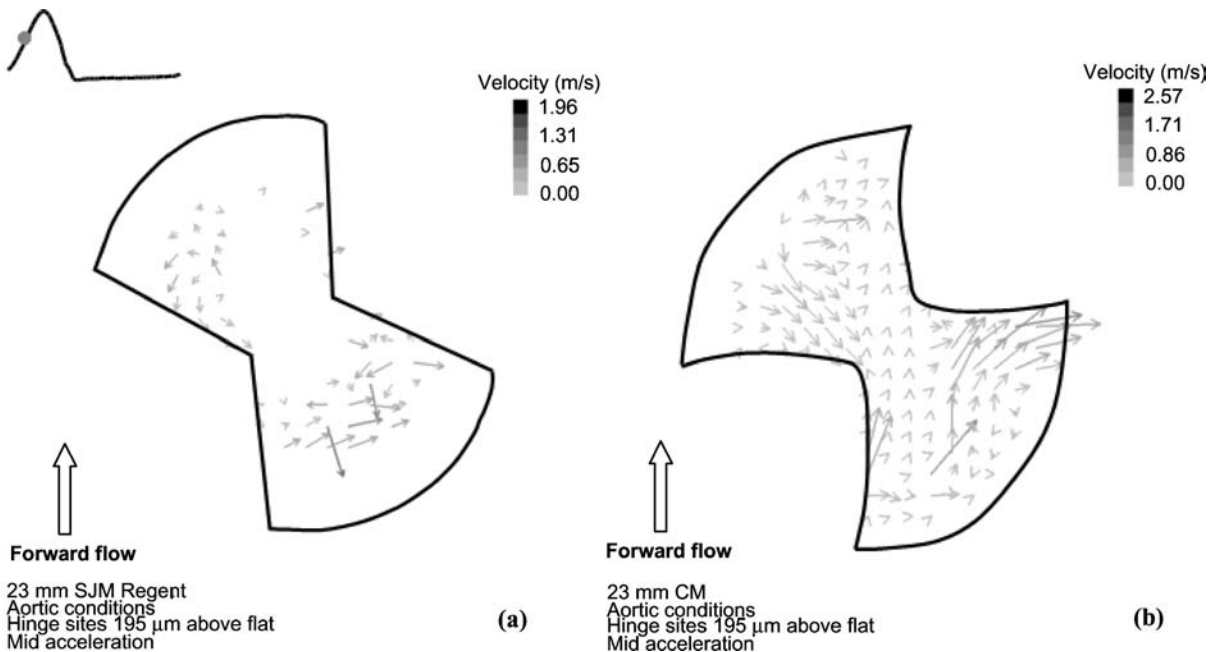

FIGURE 7. Hinge flow fields of the 23 mm SJM Regent valve (a) and of the 23 mm CM valve (b) placed in the aortic position at mid-systolic acceleration, at 195 μm above the flat level.
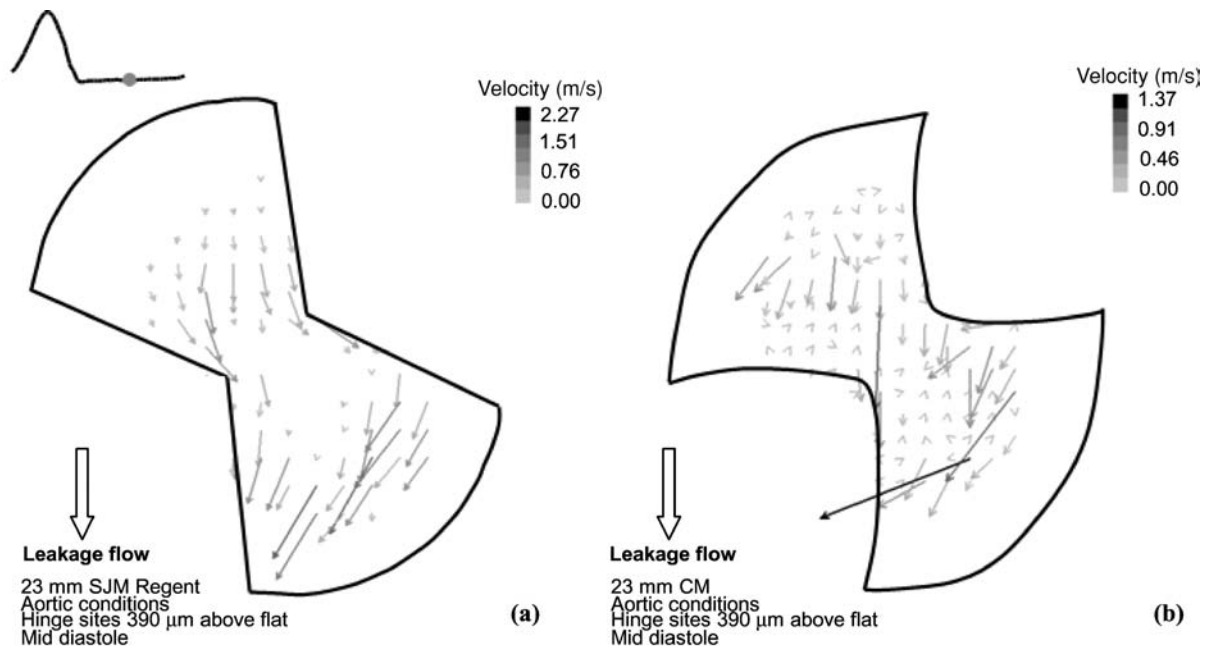
FIGURE 8. Hinge flow fields of the 23 mm SJM Regent valve (a) and of the 23 mm CM valve (b) placed in the aortic position at mid-diastole, at 390 μm above the flat level.

of 0.67 and 0.35 m/s in the adjacent corner of the SJM and CM hinges, respectively. The velocity field inside the outflow hinge pocket was nearly stagnant in both designs. During systole, the RSS levels reached 4,379 dyn/cm^2 in the CM hinge but did not exceed 779 dyn/cm^2 in the SJM hinge.

During diastole, reverse flow was observed throughout both hinge recesses but, as shown in Fig. 8, the flow pattern was different in the CM and SJM hinge designs. In the SJM hinge, leakage flow from the outflow pocket flowed around the leaflet ear before being redirected towards the ventricular corner. In the CM hinge, elevated velocity magnitudes were recorded along the inner surface of the closed leaflet in the aortic and adjacent corners. The existence of high velocities in this region could be explained by the fact that the fluid was directed over the top of the leaflet ear, as suggested by the direction of the velocity vectors. In both hinges, the maximum velocities were recorded during diastole in the ventricular corner with peak velocities of 2.27 m/s in the SJM valve and 1.37 m/s in the CM hinge.

Below the Flat Level

The flow fields were examined 1,000 μm below the flat level for both the SJM and CM hinges, with additional measurements taken 500 and 3,000 μm below the flat level in the SJM design. The flow patterns at these additional elevations were similar to those seen at 1,000 μm below the flat level.

The flow fields in Fig. 9, recorded 1,000 μm below the flat level, show a forward flow jet developing in the hinge region between the leaflets during mid-acceleration with maximum velocity magnitudes reaching 2.43 and 2.98 m/s in the SJM and CM valves, respectively. In the outflow hinge pocket, at the outside edge of the leaflets, lower peak velocities reaching 1.79 m/s in the SJM valve and 2.67 m/s in the CM design were recorded. Within the SJM thumbnail, the forward flow jet velocity decreased as the flow separated and detached from the thumbnail surface. The forward flow jet through the thumbnail region was slightly diminished and skewed towards the inner surface of the left leaflet. The forward flow was bounded by two counter rotating structures with velocity magnitudes on the order of 0.2 m/s. Higher velocity flow reaching 2 m/s was seen adjacent to these rotating flow structures.

At peak systole, the flow fields were similar to those shown in Fig. 9 at mid-acceleration, but the velocity magnitudes were lower. Between the open leaflets, in the hinge region, the peak velocity magnitudes reached 2.07 and 2.50 m/s in the SJM and CM valves, respectively. At the outside edge of the leaflets, the peak velocities were 1.69 m/s for the SJM valve and 1.80 m/s in the CM valve. Within the thumbnail of the SJM valve, the maximum central jet velocity reached 2.04 m/s. The rotating structure on the right side of the forward jet was not observed, but the velocities in this region remained low. A small low velocity recirculation region was still evident on the left of the forward flow jet.

In the CM valve design, the peak systolic RSS was recorded at the edge of the central jet between the open leaflets, whereas in the SJM valve design, the maximum RSS levels was recorded at the edge of the central jet within the thumbnail region.
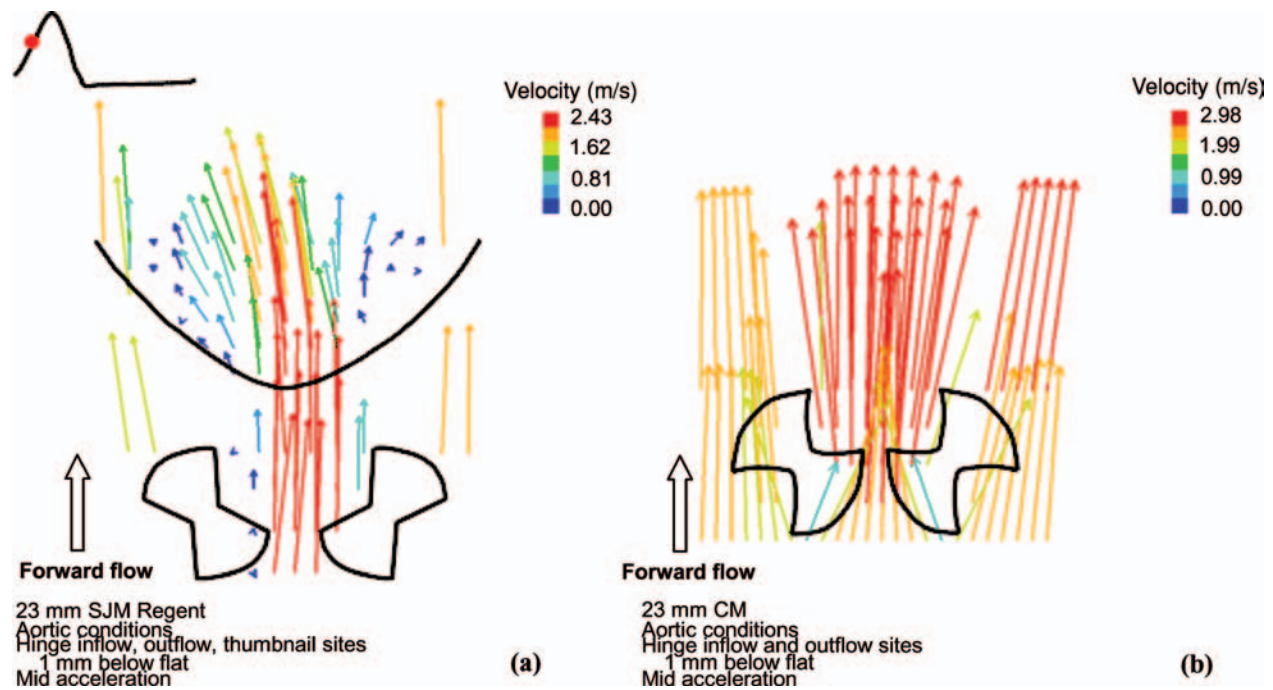
FIGURE 9. Near hinge flow fields of the 23 mm SJM Regent valve (a) and of the 23 mm CM valve (b) placed in the aortic position at mid-systolic acceleration, at 1,000 μm below the flat level.

During diastole, not shown, the entire flow fields were characterized in both valve designs by a near zero velocity reverse flow field. The velocities were <0.15 m/s except at valve closure in the CM valve design, where a velocity of 0.82 m/s was recorded in the inflow hinge pocket. The peak RSS levels were on the same order of magnitude in both valves with 864 dyn/cm^2 in the SJM valve and 842 dyn/cm^2 in the CM design.

DISCUSSION

The goal of this study was to characterize the hinge and near-hinge flow fields of the CM and the SJM Regent valve designs in the aortic position and then compare the results with previously published findings in the mitral position.[5,9] The peak velocities and RSS levels in the aortic and mitral positions within the hinge regions of the CM and the SJM valves are summarized in Tables 1 and 2, respectively.

Comparison of the SJM and CM Results

The flow fields of the SJM and CM valves under aortic conditions exhibit a number of common features; in both designs, a strong forward flow pattern and two main leakage jets were observed. However, comparison of the velocity magnitudes and RSS levels revealed some quantitative differences. Peak phase-averaged velocities measured under aortic conditions were generally higher in the CM design than in the SJM design at all considered elevations except the 390 μm level (Tables 1 and 2). Similarly, comparison

of the RSS levels revealed higher levels within the CM than within the SJM valve during the leakage phase, except at the 390 μm level. The differences in peak velocity and RSS levels may be attributed to differences in hinge geometry because the flow conditions were identical.

In the SJM valve design, the smooth streamlined hinge profile with a gradual change in geometry reduces the propensity for flow separation and turbulence. In contrast, the CM valve exhibits sharp corners that enlarge the gap available for leakage flow and an angulated recess that may disrupt the flow. Thus, the fact that the velocities and RSS levels were lower in the SJM hinge is consistent with the hinge geometry. The higher velocities and RSS levels recorded in the CM valve indicate that blood elements passing through the hinge may experience more severe flow con-

TABLE 1. Peak phase-averaged velocities and RSS levels (given in parenthesis) measured within the hinge region of the 23 mm CM valve under aortic and mitral conditions. The velocities are expressed in m/s and the RSS levels in dyn/cm^2.

Elevation	Aortic position		Mitral position[9]	
	F.F.	L.F.	F.F.	L.F.
390 μm above flat	0.73 (4380)	1.37 (4340)	0.30	2.52 (4380)
195 μm above flat	1.55 (2330)	2.57 (6190)	0.77	2.91 (5640)
Flat level	2.31 (6900)	3.08 (5440)	0.54	3.17 (5510)
1,000 μm below flat	2.98 (5880)	0.82 (840)	1.0	0.5 (4810)

Note: F.F., forward flow phase; L.F., leakage flow phase.

TABLE 2. Peak phase-averaged velocities and RSS levels (given in parenthesis) measured within the hinge region of the 23 mm SJM Regent valve under aortic and mitral conditions. The velocities are expressed in m/s and the RSS levels in dyn/cm^2.

Elevation	Aortic position		Mitral position[5]	
	F.F	L.F.	F.F.	L.F.
585 μm above flat	0.32 (260)	0.49 (650)	0.08	0.60 (2600)
390 μm above flat	1.07 (780)	2.27 (7900)	0.20	1.52 (1000)
195 μm above flat	1.04 (935)	1.96 (5460)	0.15	0.95 (700)
Flat level	1.75 (1330)	1.64 (2660)	0.13	0.72 (700)
500 μm below flat	2.49 (3190)	0.14 (1235)	0.85	0.40 (400)
1,000 μm below flat	2.43 (3190)	0.15 (865)	1.18	0.40 (600)
3,000 μm below flat	2.62 (4545)	0.15 (50)	1.10	0.20 (450)

Note: F.F., forward flow phase; L.F., leakage flow phase.

ditions, and consequently, the CM hinge may have a higher thromboembolic potential than the SJM hinge.

A number of previous studies have investigated the influence of the geometry on hinge flow fields in the mitral position. [3,5,6,9,13] Leo concluded that the flow velocity magnitudes and RSS levels in the CM valve design are greater than those of the SJM valve design.[9] The results of the present study correlate well with Leo's conclusions and emphasize the effect of the hinge geometry on the flow structures and thus on the clinical success of a bileaflet mechanical heart valve.

Comparison of Flow Fields in the Aortic and Mitral Positions

Comparison of the forward Flow Phase

Comparison of the velocity flow fields under aortic and mitral conditions during the forward flow phase revealed that below the flat level the flow features were similar. The SJM valve exhibited similar flow pattern in both positions with the preferential skewing of the jet and the regions of separated flow that persisted in the thumbnail region. Below the flat level, the flow pattern in the CM and SJM designs appeared to be, in both the aortic and mitral positions, dependent on the leaflet position. At and above the flat level, in both designs the flow was more dynamic under aortic conditions with a strong forward flow jet developing in the outflow pocket and a swirling structure in the inflow pocket.

The results compiled in Tables 1 and 2 show that the peak phase-averaged forward flow velocities were higher in the aortic position than in the mitral position for both valve designs. This difference in peak velocity level is consistent with the difference in the cardiac flow rate at these two positions, as illustrated in Fig. 1. Indeed, the peak forward flow rate is nearly twice as high in the aortic position (25 L/min) than in the mitral position (12 L/min). Because identical valves were used in both studies, the higher peak forward flow rate in the aortic position is

expected to result in higher peak forward flow velocities. Additionally, because systole is approximately half as long as diastole, the peak forward flow rate is reached in a shorter period of time in the aortic position, as shown in Fig. 1. Consequently, the fluid flowing through the aortic valve is subjected to a greater acceleration.

The differences in velocity magnitude in the aortic and mitral positions were not as marked above; the flat level as they were below the flat level for both the SJM Regent and the CM valves. This may be because the majority of the flow during the forward flow phase passed between the open leaflets, and the flow was not forced through the hinge recess. The increased resistance in the hinge region reduced the effect of the differences in forward flow rate. The higher forward aortic flow rate, leading to elevated forward flow velocities in the hinge recess, may reduce blood element buildup and ensures better wash out of the hinge region during the forward flow phase in the aortic position when compared with the mitral position.

Because the RSS levels under mitral conditions are usually lower during diastole than systole, only the RSS levels recorded during the leakage flow phase, systole in the mitral position, were published by Ellis and Leo.[5,9] Therefore, complete comparison of the RSS levels in the aortic and in the mitral positions throughout the cardiac cycle was not possible.

Comparison of the results shown in Tables 1 and 2 reveals higher peak RSS in the aortic position than the maximum levels reported in the mitral position for both valve designs, with the exception of 585 μm above the flat in the SJM Regent valve and 195 μm above the flat level in the CM valve. Since, as discussed earlier, the velocities and accelerations within the hinge recess in the aortic position were higher than those in the mitral position, higher velocity gradients and thus shear stress levels were expected in the aortic than in the mitral position during the forward flow phase.

The results obtained within the SJM design revealed that the peak RSS levels were approximately 10 times higher in the aortic position than those found by Ellis[5] in the mitral position. This larger than expected discrepancy may be due to differences in the measurement grid resolution between the grid in the present study and that in Ellis' work. The spatial resolution in regions where complex flow structures associated with high velocity gradients are expected should be able to provide a detailed and accurate representation of the flow profile. At the flat level and above, only few locations were investigated by Ellis,[5] thus, the chosen grid may not have been adequate to accurately capture the flow pattern and high RSS levels. This would explain the great difference observed between the results obtained in the current study in the aortic position and the previous mitral results.

During the forward flow phase, the peak RSS in the aortic position were generally higher than the maximum levels reported in the mitral position. Nonetheless, two factors are

thought to be critical in shear stress-induced blood damage: shear stress levels and exposure time.[10,12,17] Because diastole is half as long as systole, the difference in exposure time for the two positions has to be considered when assessing the thrombogenic potential of valve implants.

Comparison of the Leakage Flow Phase

Comparison of the flow fields found in the current study with those found by Ellis and Leo[5,9] in the mitral position revealed that the general flow features were similar during the leakage flow phase. In both positions, the flow within the hinge recess was characterized by the presence of a low reverse flow velocity and two main leakage jets, whereas below the flat level, the flow was nearly stagnant at all investigated locations.

In contrast to the forward flow phase, the peak phase-averaged leakage flow velocities in the CM design, shown in Table 1, were higher in the mitral position than in the aortic position at all investigated elevations with the exception of 1,000 μm below the flat level. The pressure gradient across the valve was greater under mitral conditions. Thus, the difference in peak leakage velocity magnitudes between aortic and mitral positions is consistent with the difference in transvalvular pressure gradient.

However, above the flat level of the SJM Regent hinge, the leakage velocity magnitudes were typically higher in the aortic than in the mitral position (Table 2). Due to the difference in transvalvular pressure, higher velocity magnitudes were expected in the mitral position. However, as discussed previously, this discrepancy may be attributed to a low spatial resolution in the mitral study. Below the flat level of the SJM Regent hinge, the velocity magnitudes were higher in the mitral than in the aortic position (Table 2). At these elevations, the flow was outside the restricted region of the hinge, and a more uniform velocity profile was expected. Thus, the spatial resolution may have a reduced effect on the results. The measurement grids in the present study and in the work of Ellis[5] were similar at levels below the flat and thus the results are consistent with those found for the CM valve.

These peak leakage velocities suggest that in both hinge designs the higher transvalvular pressure conditions in the mitral position result in higher velocity magnitudes during the closing phase than in the aortic position.

The RSS levels listed in Table 1 show that the peak RSS values in the CM hinge during the leakage phase were lower in the aortic position than in the mitral position at all elevations with the exception of 195 μm above the flat level. Similarly, the results compiled in Table 2 for the SJM Regent design show that the RSS levels during the leakage phase were higher in the aortic than in the mitral position at all elevations except at the 3,000 and 585 μm levels. As discussed previously, the elevated RSS levels found by Ellis may be attributed to the coarse measurement grid, and

therefore, direct comparison of the RSS levels may not be appropriate.

Higher RSS levels were expected in the mitral than in the aortic position due to the harsh transmitral pressure conditions during the leakage phase. The elevated velocities and RSS levels recorded under mitral conditions may enhance the thrombogenic potential of the valve and thus explain the valve's diminished clinical performance in the mitral position.

LIMITATIONS

A number of experimental factors, detailed below, limited the extent of this investigation and did not permit a more detailed interrogation of the hinge regions. The proximity of the hinges to the outer surface of the valve chamber and the motion of the leaflets within the hinge region prevented the use of three-component LDV technique. Nevertheless, the complex geometry formed by the mating of the hinge and leaflet as well as the captured hinge flow fields strongly suggest that the confined flow within the hinge recess is three-dimensional.

LDV is an inherently eulerian technique and measurements were only conducted at selected locations. Thus, the ability of this technique to resolve flow structures is limited by the measurement grid. Other experimental methods such as micro Particle Image Velocimetry, high-speed flow visualization, or the use of scale-up valve models may be used as complementary techniques to get a more detailed and complete representation of the flow fields. Additionally, in order to fully assess the thrombogenic potential of the valve implants, both the levels of shear stress a cell is exposed to and the exposure duration should be considered. A lagrangian measurement technique, such as particle tracking technique, is required to fully evaluate the exposure time of blood elements to elevated shear stress levels.

CONCLUSIONS

This study examined the flow structures within and in the vicinity of the hinges of the 23 mm CM and the 23 mm SJM Regent valves under physiological aortic conditions. Within the restricted hinge geometry of both designs, the flow fields were found to be complex and unsteady. Throughout the cardiac cycle, higher velocities as well as higher RSS levels were recorded in the CM than in the SJM valve design. These findings suggest that, when compared with the CM design, the SJM design has a superior hemodynamic performance. The streamlined smooth SJM hinge geometry may explain the better hemodynamic performance of the SJM valve when compared with that of the CM valve.

Comparison of the flow fields of the CM and SJM designs in the aortic position with results previously published in the mitral position revealed the presence of a strong forward flow pattern in the aortic position. This flow pattern

may ensure an effective wash out of the hinge region and thus limit the propensity for blood element buildup. The relatively low velocities and RSS levels recorded during the leakage flow phase in the aortic position are expected to contribute to the clinically observed higher rates of success of the aortic implants compared with the mitral implants. In contrast, the higher transmitral pressure conditions may enhance the thrombogenic potential of mitral valve implants.

The results of this study indicate that the geometry of the hinge region as well as the implant location are two critical valve design parameters. In order to achieve further reductions of thrombosis rates and to limit the need for lifelong anticoagulation therapy, importance of the implant location may have to be emphasized in future valve designs. Aortic valves are usually smaller than mitral valves; therefore, comparison of valves with identical design but with different diameters implanted in different positions may have to be pursued to fully understand the clinical performances of bileaflet mechanical heart valves implanted in the aortic and mitral positions.

ACKNOWLEDGMENTS

REFERENCES

[1] Aagaard, J., J. Tingleff, P. V. Andersen, and C. N. Hansen. Fourteen years' experience with the CarboMedics valve in young adults with aortic valve disease. *J. Heart Valve Dis.* 12(1):81–86, 2003.

[2] Bonow, R. O., B. Carabello, A. C. de Leon, L. H. Edmunds, B. J. Fedderly, M. D. Freed, W. H. Gaasch, C. R. McKay, R. A. Nishimura, P. T. O'Gara, R. A. O'Rourke, S. H. Rahimtoola, J. L. Ritchie, M. D. Cheitlin, K. A. Eagle, T. J. Gardner, A. Garson, R. J. Gibbons, R. O. Russell, T. J. Ryan, and S. C. Smith. ACC/AHA guidelines for the management of patients with valvular heart disease. Executive summary. *J. Heart Valve Dis.* 7:672–707, 1998.

[3] Ellis, J. T., T. M. Healy, A. A. Fontaine, R. Saxena, and A. P. Yoganathan. Velocity measurements and flow pattern within the hinge region of a medtronic parallel bileaflet mechanical heart valve with clear housing. *J. Heart Valve Dis.* 5(6):591–599, 1996.

[4] Ellis, J. T. An *in vitro* investigation of the leakage and hinge flow fields through bileaflet mechanical heart valves and their relevance to thrombogenesis. *PhD Thesis*, Georgia Institute of Technology, 1999.

[5] Ellis, J. T., B. R. Travis, and A. P. Yoganathan. An *in vitro* study of the hinge and near-field forward flow dynamics of the St Jude Medical Regent bileaflet mechanical heart valve. *Ann. Biomed. Eng.* 28:524–532, 2000.

[6] Ellis, J. T., and A. P. Yoganathan. A comparison of the hinge and near-hinge flow fields of St. Jude Medical Hemodynamic Plus and Regent bileaflet mechanical heart valve. *J. Thorac. Cardiovasc. Surg.* 119(1):83–93, 2000.

[7] Gross, J. M., M. C. Shu, F. F. Dai, J. T. Ellis, and A. P. Yoganathan. A microstructural flow analysis within a bileaflet mechanical heart valve hinge. *J. Heart Valve Dis.* 5(6):581–590, 1996.

[8] Krautzberger, W., D. Clevert, H. Keilbach, H. O. Kleine, C. Grosse-Siestrup, K. Affeld, E. Henning, H. Klass, V. Unger, and E. S. Bücherl. Cardiac output and right atrial pressure in long surviving animals after total heart replacement. *ESAO Proc.* 4:294–302, 1978.

[9] Leo, H. W., Z. He, J. T. Ellis, and A. P. Yoganathan. Microflow fields in the hinge region of the CarboMedics bileaflet mechanical heart valve design. *J. Thorac. Cardiovasc. Surg.* 124(3):561–574, 2002.

[10] Lu, P. C., H. C. Lai, and J. S. Liu. A reevaluation and discussion on the threshold limit for hemolysis in a turbulent shear flow. *J. Biomech.* 34(10):1361–1364, 2001.

[11] Minakata, K., Y. X. Wu, K. J. Zerr, G. L. Grunkemeier, J. R. Jr. Handy, A. Ahmad, A. Starr, and A. P. Furnary. Clinical evaluation of the CarboMedics prosthesis: Experience at Providence Health System in Portland. *J. Heart Valve Dis.* 11(6):844–850, 2002.

[12] Sallam, A. M., and N. H. C. Hwang. Human red blood cell hemolysis in a turbulent shear flow: Contribution of Reynolds shear stresses. *Biorheology* 21:783–797, 1984.

[13] Saxena, R., J. Lemmon, J. T. Ellis, and A. P. Yoganathan. An *in vitro* assessment by means of laser Doppler velocimetry of the Medtronic advantage bileaflet mechanical heart valve hinge flow. *J. Thorac. Cardiovas. Surg.* 126(1):90–98, 2003.

[14] Skoularigis, J., M. R. Essop, D. Skudicky, S. J. Middlemost, and P. Sareli. Frequency and severity of intravascular hemolysis after left-sided cardiac valve replacement with Medtronic Hall and St. Jude Medical prostheses, and influence of prosthetic type, position, size, and number. *Am. J. Cardiol.* 71:587–591, 1993.

[15] Travis, B. R. The effects of bileaflet prosthesis pivot geometry on turbulence and blood damage potential. *PhD Thesis*, Georgia Institute of Technology, 2001.

[16] Vallana, F., S. Rinaldi, P. M. Galleti, A. Nguyen, and A. Piwnica. Pivot design in bileaflet valves. *ASAIO J.* 38:M600–M606, 1992.

[17] Wurzinger, L., W. R. Opitz, M. Wolf, and H. Schmid-Schonbein. Shear-induced platelet activation: A critical reappraisal. *Biorheology* 22:399–413, 1985.